Laser and Particle Beams (2010), *28*, 319–325.
© Cambridge University Press, 2010 0263-0346/10 $20.00
doi:10.1017/S0263034610000248

Collimated proton beam generation from ultraintense laser-irradiated hole target

X.H. YANG,[1] Y.Y. MA,[1,2,3] F.Q. SHAO,[1] H. XU,[4] M.Y. YU,[5,6] Y.Q. GU,[2] T.P. YU,[1] Y. YIN,[1] C.L. TIAN,[1] AND S. KAWATA[3]

[1]Department of Physics, National University of Defense Technology, Changsha, China
[2]Laser Fusion Research Center, China Academy of Engineering Physics, Mianyang, China
[3]Center for Optical Research and Education, Graduate School of Engineering, Utsunomiya University, Utsunomiya, Japan
[4]National Laboratory Parallel and Distributed Processing, National University of Defense Technology, Changsha, China
[5]Department of Physics, Institute for Fusion Theory and Simulation, Zhejiang University, Hangzhou, China
[6]Institut für Theoretische Physik I, Ruhr-Universität Bochum, Bochum, Germany

(RECEIVED 6 January 2010; ACCEPTED 13 March 2010)

Abstract

Collimated proton beams from laser interaction with a slab having a hole on its backside are investigated using particle-in-cell simulation. The hot target electrons driven by the laser expand rapidly into the hole. However, at the hole's corners the electrons are strongly compressed and an intense electron jet is emitted from each corner, tightly followed by the ions. The plasma jets focus and collimate along the axis of the hole and can propagate without divergence within the hole. The effect of the hole diameter on the collimated proton beam is considered.

Keywords: Collimated proton beam; Hole target; PIC; Plasma jets; Ultraintense laser

1. INTRODUCTION

Recent research has demonstrated that energetic protons with multi-MeV energies can be obtained from ultraintense short laser pulse irradiation of thin targets (Okiharal *et al.*, 2002; Kaluza *et al.*, 2004; D'Humières *et al.*, 2005; Schwoerer *et al.*, 2007; Hegelich *et al.*, 2006; Ceccotti *et al.*, 2007; Yin *et al.*, 2008; Klimo *et al.*, 2008; Láska *et al.*, 2008; Bin *et al.*, 2009; Yu *et al.*, 2009a; Wang *et al.*, 2009). Such proton beams have a wide range of applications, including particle accelerators (Clark *et al.*, 2000; Nickles *et al.*, 2007; Andreev *et al.*, 2009), inertial confinement fusion (Borghesi *et al.*, 2006; Hora, 2009), laboratory astrophysics (Remington *et al.*, 1999; Borghesi *et al.*, 2002; Grun *et al.*, 2003), medical therapy (Ledingham *et al.*, 2003; Pegoraro *et al.*, 2004), etc. However, the proton beams from the laser-plasma interaction are usually divergent and not monoenergetic, and for most applications it is essential to reduce and control of the proton beam divergence and energy spread.

Much research has been devoted to improving the proton beam quality. For example, Wilks *et al.* (2001) used particle-in-cell (PIC) simulation to show that a target having a concave backside surface can result in more collimated and energetic protons. To reduce the transverse edge fields of the electron and ion clouds, Sonobe *et al.* (2005) and Nakamura *et al.* (2007) investigated laser interaction with thin foils having a hole on the backside. It is found that collimated proton beams can be obtained by controlling the transverse profile of the electron cloud. Quasimonoenergetic proton beams from the interaction of lasers with tailored hole targets have also been considered (Robinson *et al.*, 2007). Okada *et al.* (2006) considered laser interaction with concave triangular, circular, and parabolic targets, and found that the parabolic target is most suitable for accelerating protons. Liu *et al.* (2008) also considered laser interaction with parabolic targets and obtained a thin needle-profiled ion bunch. Ma *et al.* (2009) showed that high-quality collimated proton beams can be produced from the interaction of intense laser pulses with umbrellalike targets. Toncian *et al.* (2006) made use of the transient radial electric fields triggered on the inner walls of a hollow microcylinder by an intense subpicosecond laser pulse to simultaneously focus and control the energy of high-current MeV proton beams. Kar *et al.* (2008) introduced rectangular and cylindrical lens-like targets to improve the collimation of proton beams by self-charging of the target

Address correspondence and reprint requests to: Y.Y. Ma, Department of Physics, National University of Defense Technology, Changsha 410073, China. E-mail: plasim@163.com

https://doi.org/10.1017/S0263034610000248 Published online by Cambridge University Press

without the auxiliary laser pulse of Toncian *et al.* (2006). Yu *et al.* (2009b) obtained monoenergetic proton beams by laser impact with a small thin holed target, whose thickness and hole depth are only one wavelength and the hole diameter is two wavelengths. However, all these target profiles result in proton beams that become divergent shortly after the focusing.

In the classical target normal sheath acceleration (TNSA) process (Wilks *et al.*, 2001), an ultraintense laser pulse ionizes the front side of a solid target, the electrons there are pulled out, heated, and accelerated by the laser. The energetic hot electrons can propagate through the target and form an intense electrostatic sheath field at its rear side, which can reach the TV/m level. This sheath electric field accelerates the protons on the target backside. One can thus expect that a hole in the target backside should confine the expelled electrons and generate a higher sheath field. In this paper, we use the 2D3V relativistic electromagnetic collisional PIC code PLASMA SIMULATOR (PLASIM) (Ma *et al.*, 2006) to study the generation of focused and collimated protons from such a rear-holed target, sketched in Figure 1. It is found that the accelerated hot electrons indeed form an intense electrostatic sheath in the backside hole. Two focused jets of high-energy protons are ejected from the corners of the hole and merge into a high quality collimated MeV proton bunch. The latter can propagate a relatively long distance in the hole cavity since the bunch is almost neutralized by the thermal electrons there.

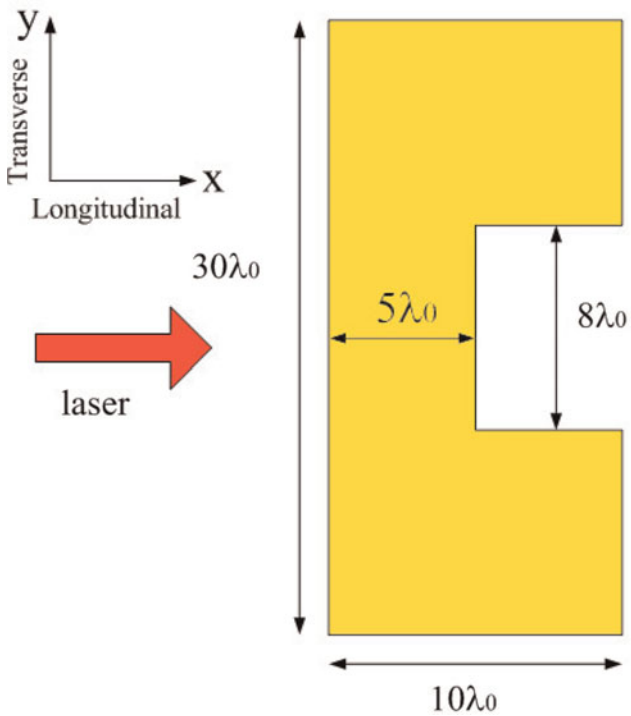


Fig. 1. (Color online) Scheme of the rear hole target. The target has a thickness of $5\lambda_0$ and is located between $x = 25\lambda_0$ and $35\lambda_0$. The laser irradiates on the target from the left side.

2. SIMULATION MODEL AND RESULTS

For our simulation, the thickness of the target is $5\lambda_0$, the depth and diameter of the hole are $5\lambda_0$ and $8\lambda_0$, respectively, where $\lambda_0 = 0.8$ μm is the laser wavelength. The simulation box is $60\lambda_0$ in the x direction and $30\lambda_0$ in the y direction. There are 1024×512 grids, and 6×10^6 particles per species. A p-polarized laser pulse is incident normally from the left side of the simulation box. The Gaussian laser envelope is given by the laser parameter $a = a_0 \exp[-(t - t_0)^2/\tau^2]\exp[-(y - y_0)^2/\sigma^2]$, where $\tau = 10T$ is the pulse width, $\sigma = 10\lambda_0$ is the spot radius, and T is the light wave period, $t_0 = 2.5\tau$, and $y_0 = 15\lambda_0$. The peak amplitude is $a_0 = 4.83$, corresponding to an intensity $I_0 = 5.0 \times 10^{19}$ W/cm^2. The hydrogen target plasma has a density of $10n_c$, where $n_c = 1.74 \times 10^{21}$ cm^{-3} is the critical density. The initial temperatures of the electrons and protons are both 1 KeV and the proton-to-electron mass ratio is $m_p/m_e = 1836$. The lateral and left boundary conditions are periodic and Lindman-absorbing, respectively.

Figure 2 for the electron density distribution shows that the target-front electrons heated and accelerated by the incident laser penetrate through the target and form an electron cloud at the rear side. For clarity, the color scale is chosen such that only the electrons in the above-critical-density regions are emphasized. We see that the less energetic electrons that remain inside the target are strongly compressed at the corners and along the horizontal hole surfaces of the hole, and the density there can exceed $15n_c$. The electrons already in the cavity but still near the hole surface can be more than $5n_c$. There is also a thin almost-unperturbed plasma layer just inside that hole surface, indicating that the high-density electrons in the target and in the cavity are unrelated. Because of the high compression inside the cavity surface, especially at the corners, two focusing jets of electrons are emitted from the latter into the cavity. The figure shows clearly that at $t = 66T$ (a) the electron jets have just come out of the two inner corners, and at $t = 75T$ (b) and $83T(c)$ the jets have grown in size and length. A strong space-charge field highly inhomogeneous near the inner cavity corners is generated. This field rapidly accelerates the protons in the target backside as in TNSA, except that here, because of the geometry and the corresponding field distribution, the protons emitted from the corner regions appear as beams that focus toward the axis. Jet-like emission from sharp target corners has also been observed in inverse-cone backed targets (Ma *et al.*, 2009). The physical mechanism is somewhat similar to that of typical armor-piercing shells (Birkhoff *et al.*, 1948; Nikitin *et al.*, 2008), where the high-pressure region is generated by a detonation wave.

Figure 3 shows the evolutions of the axial (E_x, upper row) and transverse (E_y, lower row) components of the electric field. We see that E_x and E_y are of the same order and they increase with time. At $t = 58T$ the maximum of E_x is 3.49 TV/m, occurring on the laser axis, and the maximum

https://doi.org/10.1017/S0263034610000248 Published online by Cambridge University Press

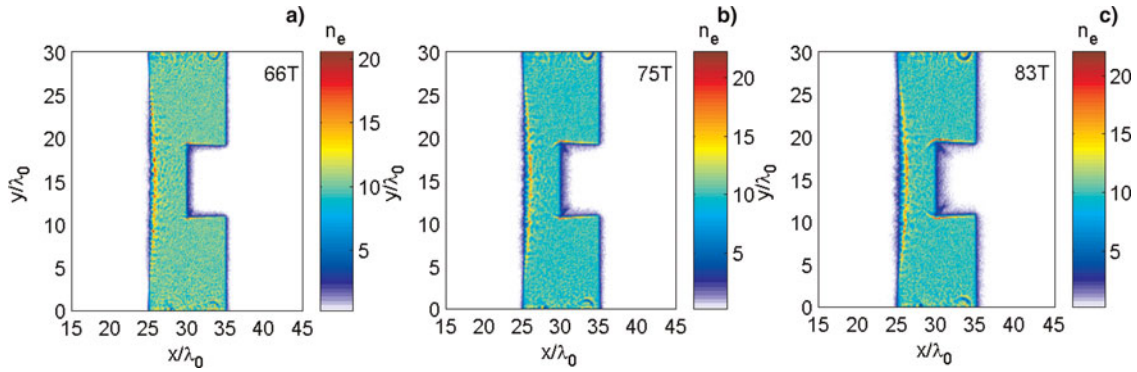


Fig. 2. (Color online) The density distributions of electrons at $t = 66T$ (**a**), $t = 75T$ (**b**), and $t = 83T$ (**c**), in units of n_c, where $n_c = 1.74 \times 10^{21}/\mathrm{cm}^3$ is the critical density.

of E_y is 3.07 TV/m, occurring at the hole inner corners. The value of the electric field agree well with the estimate obtained from the analytical formula (Mora, 2003) $E = 2E_0/(2e_N + \omega_p^2 t^2)^{1/2}$, where $E_0 = (n_{e0}k_B T_e/\varepsilon_0)^{1/2}$, n_{e0} is the initial electron density, T_e is the electron temperature, $\omega_p = (n_{e0}Ze^2/m_p\varepsilon_0)^{1/2}$ is the ion plasma frequency, and $e_N = 2.71828$. The temperature of the hot electrons can be estimated from (Wilks *et al.*, 1992) $T_e \sim \phi_p = m_e c^2\left(\sqrt{1 + I_0\lambda_0^2/2.74 \times 10^{18}\mathrm{W\mu m^2 cm^{-2}}} - 1\right)$, which is $\sim$1.31 MeV for a laser of $I = 5 \times 10^{19}\,\mathrm{W/cm^2}$ and $\lambda_0 = 0.8\,\mu\mathrm{m}$. The axial electric field in the hole is then $\sim$2.96 TV/m. The magnetic fields and plasma currents (not shown) in the target region are not significant. This can be expected since the region as well as the accelerated bunch remain nearly neutral.

In order to see the evolution of the jet-like structures, in Figure 4 we present the electron (upper row) and proton (lower row) density distributions at the later times $t = 269T$, $377T$ and $484T$. From Figures 4a and 4b, it is clear that more and more electrons are accelerated into the jets, so the diameter and density of the latter increase with time. It also can be seen that as the jets converge on the axis their directions turn into that of the laser propagation. Eventually, the two jets merge at $x \sim 33\lambda_0$, where a single electron bunch with average density $\sim 8.23n_c$ is formed. The protons also form jets whose evolution closely follows that of the electrons, as can be seen in Figures 4d and 4e.

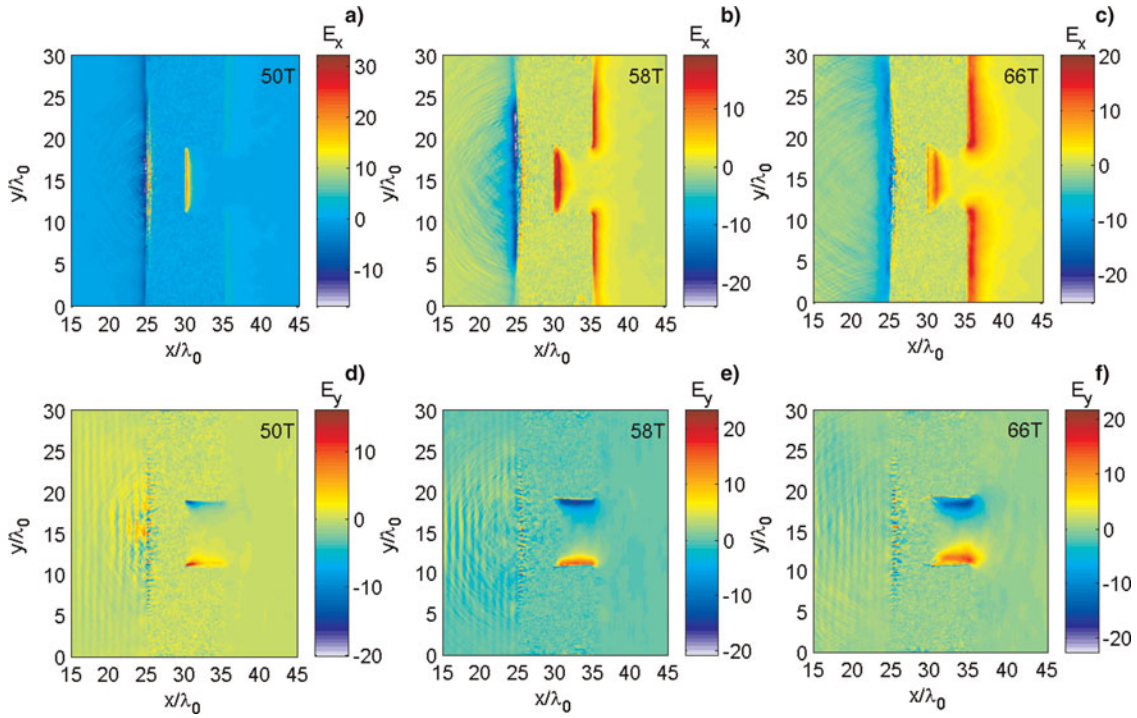


Fig. 3. (Color online) Spatial distributions of the longitudinal [(**a**), (**b**) and (**c**)] and transverse [(**d**), (**e**) and (**f**)] electric fields at $t = 50T$ [(**a**) and (**d**)], $t = 58T$ [(**b**) and (**e**)], and $t = 66T$ [(**c**) and (**f**)], in units of 1.78×10^{11} V/m.

https://doi.org/10.1017/S0263034610000248 Published online by Cambridge University Press

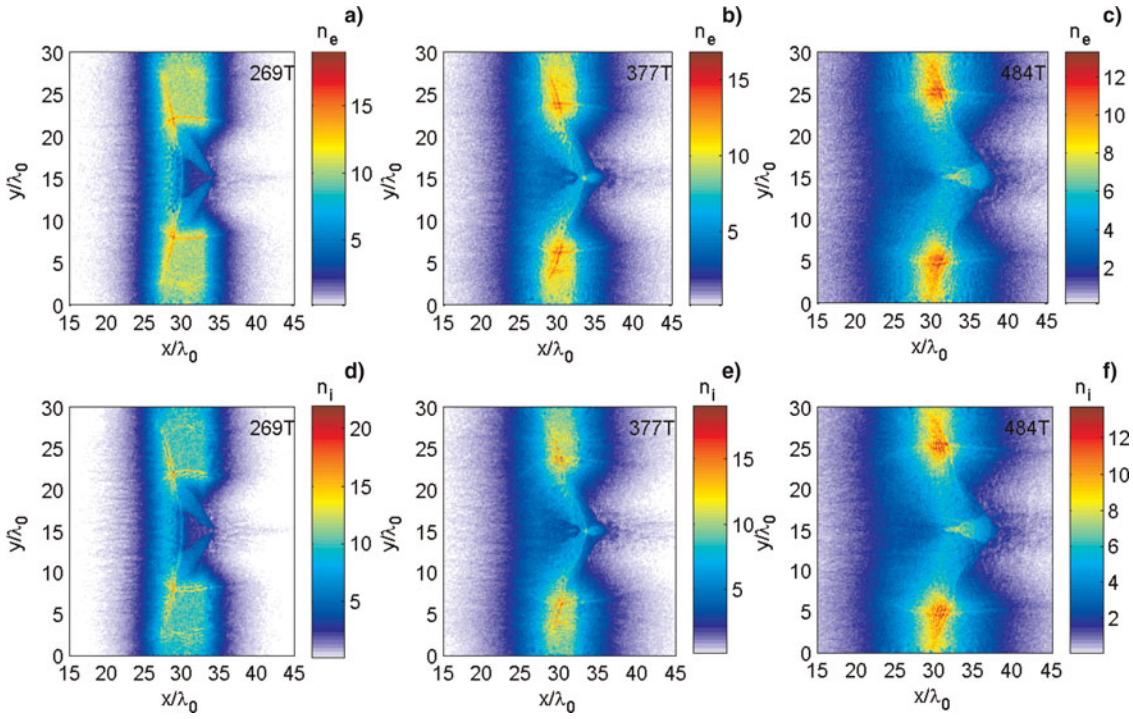


Fig. 4. (Color online) The density distributions of electrons [(**a**), (**b**) and (**c**)] and protons [(**d**), (**e**), and (**f**)] at $t = 269T$ [(**a**) and (**d**)], $t = 377T$ [(**b**) and (**e**)], and $t = 484T$ [(**c**) and (**f**)], in units of n_c, where $n_c = 1.74 \times 10^{21}/\text{cm}^3$ is the critical density.

In fact, the electron and proton jets almost overlap. That is, the accelerated bunch on the axis is almost quasineutral. The density of the bunch at $x \sim 33\lambda_0$ can reach $8.76n_c$. The collimated plasma bunch continues to move forward on the axis. Since it is continuously being fed by more and more target electrons and protons, its size increases with time. It may be of interest to mention that Sonobe *et al.* (2005) investigated proton acceleration by laser interaction with a modified double-layer scheme: using a back-holed Al foil target with a thin H layer attached to its back inside the hole. They found no evidence of plasma focusing by the hole corners. This can be attribute to the fact that their laser has a small spot (same as the transverse dimension of the hole), and the Al target is so thin ($1.5\lambda_0$ overall and $0.7\lambda_0$ up to the hole) that most of the hot electrons can pass directly into the hole, and that the much lighter protons (instead of the Al ions in the target) from the small (also same transverse dimension as the hole) attached H layer are directly driven out by TNSA into the hole.

The angular distributions of the protons in the hole before and after they merge on the axis are given in Figure 5. We see that at $t = 269T$ (black curve) the protons emitted from the two inner hole corners are confined to angles of 30°. The energetic (but low-density) protons in the axial direction are from TNSA. For the same reason the protons in the plasma bunch at later times are actually much better collimated, as can be seen in Figure 4. After the two jets collide and merge at $t = 377T$ (red curve), the emission angle of the resulting bunch is smaller, even though the emission angles of the proton jets from the corners become wider as target protons are still being accelerated into the hole. The process continues until $t = 484T$ (blue curve), when the hole structure is destroyed and the direction and profile of the corner jets become less clear. One can nevertheless see that the emission angle of the resulting proton jet actually become smaller.

The TNSA protons ejected from planar targets are normal to the back surface. With the holed target, the proton trajectories are significantly modified, as shown in Figure 6. It can be seen that typical protons are focused towards the

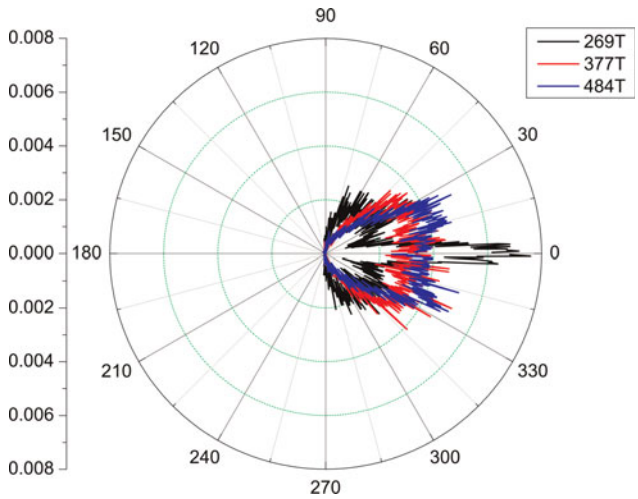


Fig. 5. (Color online) Angular distributions of protons in the hole at $t = 269T$ (black curve), $t = 377T$ (red curve) and $t = 484T$ (blue curve), respectively.

https://doi.org/10.1017/S0263034610000248 Published online by Cambridge University Press

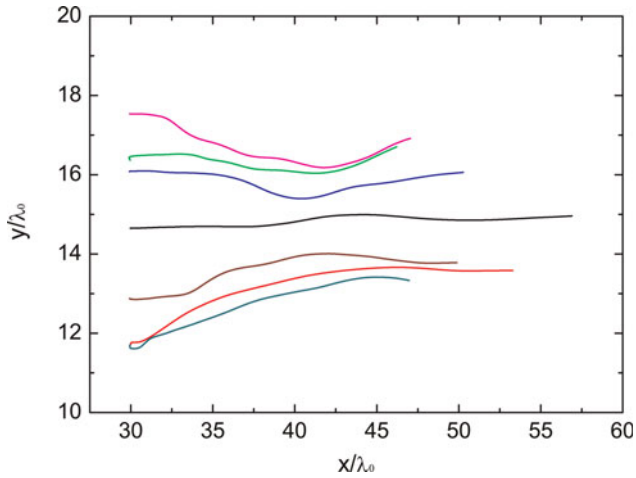


Fig. 6. (Color online) Typical proton trajectories near the hole bottom.

propagation axis, and the resulting collimated proton bunch can propagate for a much longer distance without much change. This can be attributed to the particular configuration of the space-charge field near the hole-wall as well as to the neutralization of the proton jets by the low-energy thermal electrons in the hole. At much later times, the bunch expands slowly, as seen in Figure 4f. That is, it does not diverge rapidly as for targets with smooth planar or concave backsides (Okada *et al.*, 2006; Liu *et al.*, 2008; Ma *et al.*, 2009), since the space-charge field in the hole has a guiding effect in the formation and propagation of the bunch. This can be seen in Figure 7 for the transverse momentum P_y of protons originated from the upper and lower corners, especially when they converge onto the axis. Figure 7a corresponds to Fig. 4(d), when the jets have not yet converged. We see that at that time the protons from the hole corners have larger transverse momentum, with a maximum of $P_{y\ \max} \sim 0.07 m_p c$. Fig. 7(b) shows that at $t = 377T$ $P_{y\ \max}$ decreases to $0.06 m_p c$. At $484T$, when the structure of the target has been destroyed and most of the protons have converged, we have $P_{y\ \max} \sim 0.04 m_p c$, which is nearly half that at $269T$. That is, the protons become more and more aligned to the axis. Similar results are found for the target with densities of $4n_c$, $7n_c$, $20n_c$, etc. We find that the higher the initial density of the target is, the shorter the time for the protons to converge on the axis and the higher the density of the proton bunch. However, since there are many more protons originating from the hole corners of the higher density target, the proton bunch for the $20n_c$ target is not as distinct as that for the $10n_c$ target.

3. EFFECT OF THE HOLE DIAMETER

In the proton acceleration process, appropriate laser and target parameters are crucial for the proton beam quality. In order to obtain high quality proton bunches, that is, bunches with high energy and density, and low divergence, etc., one can optimize these parameters. We now consider the effect of the hole diameter D, keeping the laser spot radius fixed at $\sigma = 10\lambda_0$. The density distributions of the proton bunch for $D = 4\lambda_0$ and $D = 12\lambda_0$ at $t = 377T$ are presented in Figures 8a and 8b, respectively. It can be seen that the larger the D, the longer the focal length and the longer the time needed for the protons to converge. For example, at $377T$ the bunch from the $D = 4\lambda_0$ target has converged but that for $D = 12\lambda_0$ has not converged. For the $D = 4\lambda_0$ target most protons from the hole corners can cross the propagation axis and are not efficiently accelerated in the axial direction. Figure 8b shows that for the $D = 12\lambda_0$ target almost all the protons from the hole corners are accelerated efficiently and focused onto the propagation axis, although the density is lower. Figure 9 gives the energy distribution of the protons in the hole for $D = 4\lambda_0$ (black curve), $D = 8\lambda_0$ (red curve), $D = 12\lambda_0$ (blue curve) at $t = 377T$. It can be seen that protons from the target with the small hole are lower in number and have lower cutoff energy. From the fact that laser spot radius is $\sigma/\sqrt{2} \approx 7\lambda_0$ here, we see that to obtain large proton current, the diameter of the hole should be about the laser spot radius. This is because for too-large diameter holes, the protons emitted from the corners need to propagate much longer distances and can thus become dispersed before they merge. The resulting bunch will then

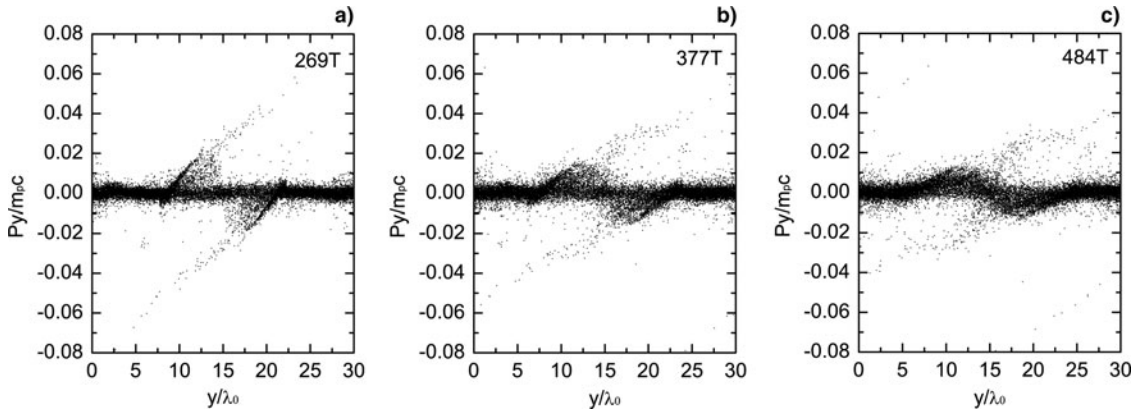


Fig. 7. Transverse momentum distributions of the protons at the time of $t = 269T$ (**a**), $t = 377T$ (**b**), and $t = 484T$ (**c**), respectively.

https://doi.org/10.1017/S0263034610000248 Published online by Cambridge University Press

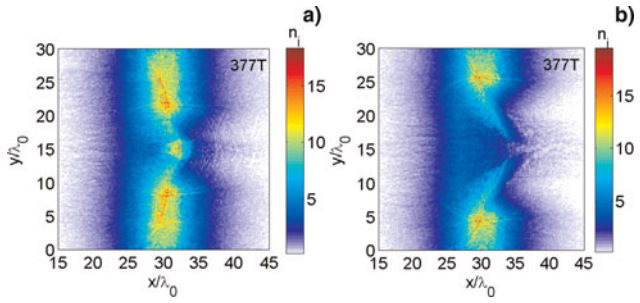


Fig. 8. (Color online) The proton density distributions for $D = 4\lambda_0$ (**a**) and $D = 12\lambda_0$ (**b**) at $t = 377T$, in units of n_c. The other parameters are the same as that in the other figures.

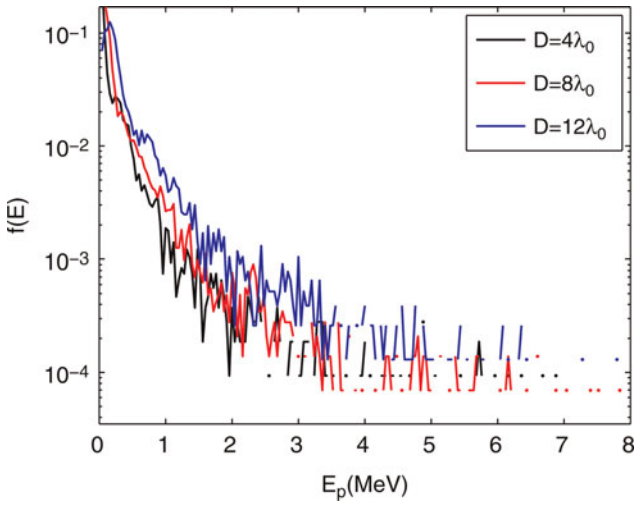


Fig. 9. (Color online) Energy spectra of the protons in the hole for $D = 4\lambda_0$ (black curve), $D = 8\lambda_0$ (red curve), $D = 12\lambda_0$ (blue curve) at $t = 377T$. The other parameters are the same as that in the other figures.

of low density and not well collimated. When the hole diameter is too small, the protons converge too early and just pass each other on the axis, since the cavity space-charge field favorable for merging and guiding of the bunch is further downstream.

4. SUMMARY

We have presented a scheme for obtaining collimated proton bunches from the interaction of an ultraintense laser pulse with a rear-holed target. Energetic electron and proton jets are generated from the inner hole corners and merge on the laser axis. The resulting quasi-neutral plasma bunch is well collimated and can propagate in the hole cavity for a long distance along the axis. It is shown that the density and current of the bunch can reach $8.76n_c$ and 1.33×10^{12} A/cm^2, respectively, and that the bunch can propagate without divergence over a longer distance in the hole. The diameter of the hole is crucial to the quality of the proton bunch. To realize large proton current, itshould be near that of the laser spot.

ACKNOWLEDGMENTS

This work was supported by the National High-Tech ICF Committee, the National Natural Science Foundation of China (10505030, 10505031, 10576035, 10605038, 10835003, 10975185, and 10976031), the Science and Technology Development Foundation of the Chinese Academy of Engineering Physics (2006Z0202), and the National Basic Research Program of China (2007CB815105, 2008CB717806 and 2009GB105005). We also acknowledge the support of the National University of Defense Technology (NUDT) Foundation (JC09-02-08) and the NUDT High Performance Computer Research Center. Y. Y. Ma acknowledges the support of the JSPS and CORE of Utsunomiya University, Japan.

REFERENCES

Andreev, A., Platonov, K. & Kawata, S. (2009). Ion acceleration by short high intensity laser pulse in small target sets. *Laser Part. Beams* **27**, 449–457.

Bin, J.H., Lei, A.L., Yang, X.Q., Huang, L.G., Yu, M.Y., Yu, W. & Tanaka, K.A. (2009). Quasi-monoenergetic proton beam generation from a double-layer solid target using an intense circularly polarized laser. *Laser Part. Beams* **27**, 485–490.

Birkhoff, G., Macdougall, D.P., Pugh, E.M. & Taylor, G. (1948). Explosives with lined cavities. *J. Appl. Phys.* **19**, 563–582.

Borghesi, M., Campbell, D.H., Schiavi, A., Willi, O., Mackinnon, A.J., Hicks, D., Patel, P., Gizzi, L.A., Galimberti, M. & Clarke, R.J. (2002). Laser-produced protons and their application as a particle probe. *Laser Part. Beams* **20**, 269–275.

Borghesi, M., Fuchs, J., Bulanov, S.V., Mackinnon, A.J., Patel, P.K. & Roth, M. (2006). Fast ion generation by high-intensity laser irradiation of solid targets and applications. *Fusion Sci. Technol.* **49**, 412–439.

Ceccotti, T., Lévy, A., Popescu, H., Réau, F., D'oliveira, P., Monot, P., Geindre, J.P., Lefebvre, E. & Martin, P. (2007). Proton acceleration with high-intensity ultrahigh-contrast laser pulses. *Phys. Rev. Lett.* **99**, 185002-1/185002-4.

Clark, E.L., Krushelnick, K., Davies, J.R., Zepf, M., Tatarakis, M., Beg, F.N., Machacek, A., Norreys, P.A., Santala, M.I.K., Watts, I. & Dangor, A.E. (2000). Measurements of energetic proton transport through magnetized plasma from intense laser interactions with solids. *Phys. Rev. Lett.* **84**, 670–673.

D'Humières, E., Lefebvre, E., Gremillet, L. & Malka, V. (2005). Proton acceleration mechanisms in high-intensity laser interaction with thin foils. *Phys. Plasmas* **12**, 062704-1/062704-13.

Grun, J., Laming, M., Manck, C., Donnelly, D.W., Covington, B.C., Fischer, R.P., Velikovich, A. & Khokhlov, A. (2003). Laser- plasma simulations of astrophysical phenomena and novel applications to semiconductor annealing. *Laser Part. Beams* **21**, 529–534.

Hegelich, B.M., Albright, B.J., Cobble, J., Flippo, K., Letzring, S., Paffett, M., Ruhl, H., Schreiber, J., Schulze, R.K. & Fernández, J.C. (2006). Laser acceleration of quasi-monoenergetic MeV ion beams. *Nature* (London) **439**, 441–444.

Hora, H. (2009). Laser fusion with nonlinear force driven plasma blocks: Thresholds and dielectric effects. *Laser Part. Beams* **27**, 207–222.

https://doi.org/10.1017/S0263034610000248 Published online by Cambridge University Press

Kaluza, M., Schreiber, J., Santala, M.I.K., Tsakiris, G.D., Eidmann, K., Meyer-Ter-Vehn, J. & Witte, K.J. (2004). Influence of the laser prepulse on proton acceleration in thin-foil experiments. *Phys. Rev. Lett.* **93**, 045003-1/045003-4.

Kar, S., Markey, K., Simson, P.T., Bellei, C., Green, J.S., Nagel, S.R., Kneip, S., Carroll, D.C., Dromey, B., Willingale, L., Clark, E.L., Makenna, P., Najmudin, Z., Krushelnick, K., Norreys, P., Clarke, R.J., Neely, D., Borghesi, M. & Zepf, M. (2008). Dynamic control of laser-produced proton beams. *Phys. Rev. Lett.* **100**, 105004-1/105004-4.

Klimo, O., Psikal, J., Limpouch, J. & Tikhonchuk, V.T. (2008). Monoenergetic ion beams from ultrathin foils irradiated by ultrahigh-contrast circularly polarized laser pulses. *Phys. Rev. ST Accel. Beams* **11**, 031301-1/031301-14.

Láska, L., Jungwirth, K., Krása, J., Krouský, E., Pfeifer, M., Rohlena, K., Velyhan, A., Ullschmied, J., Gammino, S., Torrisi, L., Badziak, J., Parys, P., Rosinski, M., Ryć, L. & Wolowski, J. (2008). Angular distributions of ions emitted from laser plasma produced at various irradiation angles and laser intensities. *Laser and Part. Beams* **26**, 555–565.

Ledingham, K.W.D., McKenna, P. & Singhal, R.P. (2003). Application for nuclear phenomena generated by ultra-intense laser. *Science* **300**, 1107–1111.

Liu, M.P., Wu, H.C., Xie, B.S., Liu, J., Wang, H.Y. & Yu, M.Y. (2008). Energetic collimated ion bunch generation from an ultra-intense laser interacting with thin concave targets. *Phys. Plasmas* **15**, 063104-1/063104-8.

Ma, Y.Y., Sheng, Z.M., Gu, Y.Q., Yu, M.Y., Yin, Y., Shao, F.Q., Yu, T.P. & Chang, W.W. (2009). High-quality MeV protons from laser interaction with umbrellalike cavity target. *Phys. Plasmas* **16**, 034502-1/034502-4.

Ma, Y.Y., Sheng, Z.M., Li, Y.T., Chang, W.W., Yuan, X.H., Chen, M., Wu, H.C., Zheng, J. & Zhang, J. (2006). Dense quasi-monoenergetic attosecond electron bunches from laser interaction with wire and slice targets. *Phys. Plasmas* **13**, 110702-1/110702-4.

Mora, P. (2003). Plasma expansion into a vacuum. *Phys. Rev. Lett.* **90**, 185002-1/185002-4.

Nakamura, M., Kawata, S., Sonobe, R., Kong, Q., Miyazaki, S., Onuma, N. & Kikuchi, T. (2007). Robustness of a tailored hole target in laser-produced collimated proton beam generation. *J. Appl. Phys.* **101**, 113305-1/113305-7.

Nickles, P.V., Ter-Avetisyan, S., Schnürer, M., Sokollik, T., Sandner, W., Schreiber, J., Hilscher, D., Jahnke, U., Andreev, A. & Tikhonchuk, V. (2007). Review of ultrafast ion acceleration experiments in laser plasma at Max Born Institute. *Laser Part. Beams* **25**, 347–363.

Nikitin, S.P., Grun, J., Aglitskiy, Y. Manka, C., Zabetakis, D., Velikovich, A.L. & Millerl, C. (2008). Production of cumulative jets by ablatively-driven implosion of hollow cones and wedges. *Phys. Plasmas* **15**, 050703-1/050703-4.

Okada, T., Andreev, A.A., Mikado, Y. & Okubo, K. (2006). Energetic proton acceleration and bunch generation by ultraintense laser pulses on the surface of thin plasma targets. *Phys. Rev. E* **74**, 026401-1/026401-5.

Okihara, S., Sentoku, Y., Sueda, K., Shimizu, S., Sato, F., Miyanaga, N., Mima, K., Izawa, Y., Iida, T. & Sakabe, S. (2002). Energetic proton generation in a thin plastic foil irradiated by intense femtosecond lasers. *J. Nucl. Sci. Technol.* **39**, 1–5.

Pegoraro, F., Atzeni, S., Borghesi, M., Bulanov, S., Esirkepov, T., Honrubia, J., Kato, Y., Khoroshkov, V., Nishihara, K., Tajama, T., Temporal, M. & Willi, O. (2004). Production of ion beams in high-power laser-plasma interaction and their application. *Laser Part. Beams* **22**, 19–24.

Remington, B.A., Arnet, D., Drake, R.P. & Takabe, H. (1999). Modeling astrophysical phenomena in the laboratory with intense laser. *Science* **284**, 1488–1493.

Robinson, A.P.L. & Gibbon, P. (2007). Production of proton beams with narrow-band energy spectra from laser-irradiated ultrathin foils. *Phys. Rev. E* **75**, 015401-1/015401-4.

Schwoerer, H., Pfotenhauer, S., Jächkel, O., Amthor, K.U., Liesfeld, B., Ziegler, W., Sauerbrey, R., Ledingham, K.W.D. & Esirkepov, T. (2006). Laser-plasma acceleration of quasi-monoenergetic protons from microstructured targets. *Nature* (London) **439**, 445–448.

Sonobe, R., Kawata, S., Miyazaki, S., Nakamura, M. & Kikuchi, T. (2005). Suppression of transverse proton beam divergence by controlled electron cloud in laser-plasma interactions. *Phys. Plasmas* **12**, 073104-1/073104-6.

Toncian, T., Borghesi, M., Fuchs, J., D'Humieres, E., Antici, P., Audebert, P., Brambrink, E., Cecchetti, C.A., Pipahl, A., Romagnani, L. & Willi, O. (2006). Ultrafast laser-driven micro-lens to focus and energy-select Mega-electron volt protons. *Science* **312**, 410–413.

Wang, X., Yu, W., Yu, M.Y., Senscha, V.K., Xu, H., Wang, J.W., Yuan, X. & Sheng, Z.M. (2009). Efficient acceleration of a small dense plasma pellet by consecutive action of multiple short intense laser pulses. *Laser Part. Beams* **27**, 629–634.

Wilks, S.C., Landon, A.B., Cowan, T.E., Roth, M., Hatchett, S., Key, M.H., Pennington, D., Mackinnon, A. & Snavely, R.A. (2001). Energetic proton generation in ultra-intense laser-solid interactions. *Phys. Plasmas* **8**, 542–549.

Wilks, S.C., Kruer, W.L., Tabak, M. & Langdon, A.B. (1992). Absorption of ultra intense laser pulse. *Phys. Rev. Lett.* **69**, 1383–1386.

Yin, L., Albright, B.J., Hegelich, B.M., Bowers, K.J., Flippo, K.A., Kwan, T.J.T. & Fernández, J.C. (2007). Monoenergetic and GeV ion acceleration from the laser breakout afterburner using ultrathin targets. *Phys. Plasmas* **14**, 056706-1/056706-8.

Yu, T.P., Chen, M. & Pukhov, A. (2009*a*). High quality GeV proton beams from a density-modulated foil target. *Laser Part. Beams* **27**, 611–617.

Yu, T.P., Ma, Y.Y., Chen, M., Shao, F.Q., Yu, M.Y., Gu, Y.Q. & Yin, Y. (2009*b*). Quasimonoenergetic proton beam from ultraintense-laser irradiation of a target with holed backside. *Phys. Plasmas* **16**, 033112-1/033112-6.

https://doi.org/10.1017/S0263034610000248 Published online by Cambridge University Press